TENSILE FRACTURE

OF

DUCTILE MATERIALS

by

Devdas Mizar Pai

A Thesis Presented in Partial Fulfillment
of the Requirements for the Degree
Master of Science

ARIZONA STATE UNIVERSITY

May 1984

TENSILE FRACTURE

OF

DUCTILE MATERIALS

by

Devdas Mizar Pai

has been approved

May 1984

APPROVED:

4/30/84, Chairperson

May 3, 1984

May 3, 1984

Supervisory Committee

ACCEPTED:

Department Chairperson

Dean, Graduate College

ABSTRACT

It has been established that for brittle materials, circular voids play an important role relative to fracture, in that they intensify both tensile and compressive stresses. A maximum intensified tensile stress failure criterion applies quite well to brittle materials.

In this thesis, an attempt has been made to explore the possibility of extending the approach to the tensile fracture of ductile materials. The three-dimensional voids that exist in reality are modelled by circular holes in sheet metal. Mathematical relationships are sought between the shape and size of the hole, after the material is plastically deformed, and the amount of deformation induced. Then, the effect of hole shape, size and orientation on the mechanical properties is considered experimentally. It is seen that the presence of the voids does not affect the ultimate tensile strength of the ductile materials because plastic flow wipes out the stress intensification caused by them. However, the shape and orientation of the defect is found to play an important role in affecting the strain at fracture. In certain engineering applications the strain at fracture is more important than the stress at fracture. The findings of this thesis have the potential of being applied to a rolling mill stiffness acceptance test and to the large strain-low stress deformation of sheet material.

ACKNOWLEDGEMENTS

Grateful acknowledgement is made of the patient and valuable guidance provided me in no small measure by Professor Milton C. Shaw during the course of this research attempt.

Financial support from the National Aeronautics and Space Administration through NASA Research Grant NAG-1-339 is gratefully acknowledged.

I am grateful to all my colleagues and professors for their valuable advice and constructive criticism. In particular, I wish to thank Mr. Ramaraj and Mr. Chandrasekar for the SEM fractographs they took for me. I also extend my thanks to the Development Shop for preparing the specimens.

Finally, I would like to express my appreciation to Mrs. Shirley Farrow for her kind cooperation in typing this report so well in such a short period of time.

TABLE OF CONTENTS

LIST OF TABLES

LIST OF FIGURES

I. INTRODUCTION

Fracture comprises the fragmentation of a solid material into two or more parts under the action of stress [1]. It can be categorised into brittle fracture and ductile fracture.

Experiments have shown an intensified stress theory to give good results when applied to brittle fracture. The intensified stress theory of Takagi and Shaw [2] assumes round rather than hairline defects and voids in the brittle materials. The purpose of the present study has been to explore the role that shaped voids play with regard to the tensile fracture of ductile materials.

This thesis concerns itself first with the change of shape of such voids when the material containing the voids is deformed plastically. The second part of the thesis is the study of the effect of void or defect shape and orientation on the tensile strength of the material and it is attempted to extend the theory of Takagi to ductile materials. A number of experiments have been conducted in relation to each part of the thesis. In these, two simplifying assumptions are made:

1. Although the defects in actual materials are liable to be relatively weak particles such as silicates or other slag particles, the defects actually studied are unfilled voids.
2. Since two dimensional (plane strain) results are generally in good agreement with more complex situations, the voids employed will be cylindrical holes in sheet material.

The voids are made to deform first by the metal forming operation of rolling, and later they deform when specimens cut out of the rolled sheets are pulled in tension. Since the stress concentration strongly depends on the shape of the void, the final shape of the void at fracture is considered in applying the intensified stress criterion to ductile materials.

II. REVIEW OF PAST WORK

Unlike ductile fractures, that exhibit significant plastic deformation, brittle fractures propagate rapidly and often with catastrophic results, with little or no plastic deformation. The tendency for brittle fractures to happen is increased with decreasing temperature, increasing strain rate, and triaxiality of stress. Dieter [1] shows the types of fractures seen in metals under uniaxial tension. In brittle fracture, separation is normal to the tensile stress (Fig. 1a). These are observed in bcc and hcp but rarely in fcc metals. Ductile fracture could be shear type (Fig. 1b), rupture (Fig. 1c) or "cup and cone" type (Fig. 1d).

Griffith [3] first considered the mechanics of brittle fracture from the point of view of crack initiation and crack propagation. He assumed the existence of a population of fine hairline cracks in brittle materials and then went on to use an energy approach to develop a crack propagation criterion. In his words, "A crack will propagate when the decrease in elastic strain energy is at least equal to the energy required to create the new crack surface." This criterion was used to obtain the fracture locus of a brittle material subjected to biaxial loading. Experiments to check the validity of this locus were performed by Takagi [2] using the four point bending test, the uniaxial compression test, and the disc test. Griffith's results were found to agree very well qualitatively but not quantitatively; assuming a circular void was found to be much better than assuming a hairline crack. One could state this new criterion

thus: "Brittle fracture will occur in tension when the maximum intensified tensile stress at a point on the periphery of the void reaches a critical value characteristic of the material."

Now, as far as ductile materials are concerned, we are well aware of the presence of inclusions such as sulfides and silicates and also porosities and other defects in the as-cast state. When the material is plastically deformed, as by rolling, the spherical particles deform into ellipsoids and this gives rise to a significant difference in mechanical properties measured parallel (longitudinal) and perpendicular (transverse) to the direction of rolling.

Extensive work has been done in the 1940s and 1950s regarding the anisotropy of mechanical properties in wrought products. Wells and Mehl [4] studied the effect of forging reduction, ingot size, yield strength, reheat treatment and nonmetallic inclusions on the transverse mechanical properties. They found the reduction of area of specimens to depend strongly on the angle between the longitudinal axis and flow direction, as seen in Fig. 2(a). Transverse properties are particularly important in thick walled tubes as in pressure vessels and guns. Transverse ductility is found to be much lower than the longitudinal ductility and this difference is due to inclusions, microsegregation and dendritic structure. These inclusions, voids and second phase particles get aligned preferentially in the direction of working, causing directional dependence of properties such as minimum reduction of area in the short-transverse direction, intermediate in the long-transverse direction and maximum in the longitudinal direction. Fig. 2(b), also

taken from [4], shows how, beyond a certain forging ratio, the inclusions get so elongated in the longitudinal direction that the transverse reduction of area property (RAT) drops off with further reduction. Grobe, Wells and Mehl [5] studied the effect of various kinds of heat treatment on SAE 1045 forging steel. These tests also show that yield strength and tensile strength are practically unaffected by the angle of the test. Loria [6] from his experiments on large steel forgings, also explains the anisotropy in properties by the "possible formation of a coarse dendritic structure in large ingots and the coalescence of inclusions which are drawn out into appreciable stringers during forging." Welchner and Hildorf [7] consider both the quantity and type of inclusions insofar as their effect on transverse mechanical properties is concerned. The more the inclusion and the lower its shape "rating", the lower was the RAT value. The type of inclusion was found to be more important than the quantity. Even in very pure single phase material like Oxygen Free High Conductivity Copper (OFHC), this anisotropy was seen by Backofen, Shaler and Hundy [8].

The mechanics of interaction of the inclusions when in certain regular patterns and the consequences on the fracture characteristics has been studied by McClintock [9], who has analytically found that rigid inclusions can cause infinite strain concentrations in the matrix near the interface while stress concentrations are about two for roughly spherical inclusions. He also finds that the stage of fracture corresponding to the homogeneous growth of holes before they coalesce to nucleate a crack is dependent on the logarithm of the

volume fraction of inclusions. Interaction of hole arrays is also an important consideration in the design of perforated plates such as those used as tube-sheets in heat exchangers [10-11]. The analysis uses theory as well as strain analysis and photoelastic tests.

Several theoretical elastic analyses have been done for the stress concentrations around spherical and spheroidal inclusions and cavities [12-15]. The results are mostly presented as graphs with the principal axes of the spheroids as parameters.

However, most of the work on void shape mentioned above deals with the elastic case only. The change in shape of round voids when the material is subjected to significant plastic deformation has also been dealt with in the literature. Johnson and Mamalis [16] have described exhaustively the range of physical defects that occur in various metalworking processes. Chaaban and Alexander [18] have studied the main factors affecting the mode of deformation, strain distribution and closure of internal cavities within a billet subjected to swing forging. Internal cavities were simulated by longitudinal and transverse holes of various sizes and dispositions machined into lead billets. Longitudinal holes were found to have a higher rate of closure than the transverse holes. Although the inner surfaces of the deformed hole came into contact, bonding was only initiated and not too strong. Chaaban and Helmi [17] simulated physical defects in hot-rolled steel by artificial longitudinal, transverse and vertical holes in plasticine [Fig. 3].

III. EXPERIMENTAL PROCEDURE

Experiments on deformation and strength were performed on 3 materials - (i) High purity OFHC Copper (ii) Aluminum alloy Al 5052 (iii) Low Carbon steel AISI 1018 cold rolled. The important properties of these materials are listed in Table 1 (after Schey [19]).

The experiments performed come under two major subheadings.

I. Shape Change Experiments:

a) Specimen preparation: Through holes of 0.015" (0.38mm) and 0.040" (1mm) diameters were drilled in strips of each of the 3 materials 4.5" (114mm) inches wide and 0.125" (3.175mm) thick. The 0.040" holes could be made perfectly round and cylindrical by reaming but this was not possible for the 0.015" holes, so the smaller size of holes were not used in subsequent experiments. The holes were drilled in two kinds of clusters (see Fig. 4): a) with centers lying along the line perpendicular to the longitudinal direction and b) with centers lying in the longitudinal direction with a spacing of 0.3" (7.62mm).

Another kind of specimen (type B, Fig.5) was made with holes just along its longitudinal axis. These strips were 2.3" (58mm) long. The holes were spaced 1.2" (30.98mm) apart. For steel alone, yet another kind of specimen was made that had holes only along its transverse axis - in type C1 there were 3 holes 1.3" (33.02mm) apart, in type C2-C4 there were 4 holes 1.0" (25.4mm) apart and the specimens were 4" (101.6mm) wide. See Fig. 6.

Interaction effects between adjacent holes were studied using a specimen having 1, 9 and 25 holes in a square arrangement. (Fig. 7).

b) Deformation: Subsequent to drilling the holes, the specimens were rolled in plane strain in a Stanat EX-100 3hp (2.24kW) rolling mill of 1.2" (30.48mm) maximum gap at 450rpm. The roll diameter was 3.085" (78.36mm). SAE30 motor oil was used as lubricant in all cases. Type A specimens were reduced in thickness by 50% in 6 passes. Type B and type C specimens were reduced in thickness by 35% in 3 passes. In all cases, after each pass, photographs were taken at 50X of all the holes in the specimens using a Leitz Metalloplan microscope with Polaroid camera, to obtain the hole size and shape at each stage.

II. Fracture Experiments

Two types of tensile specimens have been used:

a) Rectangular Tension Test Specimens: These are geometrically similar to the one specified in the ASTM standard for tension tests of metals [20]. See Fig. 8. These are cut out from specimens A and C1-C4 used in the shape change experiments. Both longitudinal and transverse specimens were obtained from A. By a longitudinal specimen is meant a specimen with its longitudinal axis parallel to the direction of rolling, while a transverse specimen is one that has its longitudinal axis perpendicular to the direction of rolling. Only longitudinal specimens were obtained from C1-C4. Some of the specimens have no holes in them. Some have elliptical holes in the center. These holes were round initially and were deformed during

rolling. The rest have round holes 0.040" (1mm) diameter drilled into them after rolling. The dimensions of the various specimens are tabulated in Table 2.

b) Plane Strain Tensile Specimens: These are of the dimensions shown in Fig. 9. These were cut out of shape change specimen type B after rolling and are also of two kinds, longitudinal and transverse. The number of specimens of each kind are listed in Table 3.

All the specimens from A and half the specimens of each kind from B and C were annealed at the appropriate temperature for the material concerned (see Table 1). Annealing was done for one hour at the specified temperature and the specimens were furnace cooled. In the case of copper, any surface oxide layer formed was removed using dilute hydrochloric acid and in the case of steel, the oxide layer was so flaky that it was just removed using fine emery paper.

The tension tests were carried out on a Model TT-D Instron Universal Testing Machine using a crosshead speed 0.05 inches/min (1.24mm/min) which corresponds to quite a low strain rate of from 0.0167/min for the longest specimens to 0.1/min for the plane strain specimens which had a gage length of 0.5 inches. Load versus displacement was recorded until the load reached a maximum. Then the machine was unloaded and the specimen width and the thickness were measured relative to size and shape of the central defect. The specimen was then returned to the machine and tested to fracture so that the size and shape of the final fracture surface could be determined.

Typical microstructures of the 3 materials in the annealed state were obtained by mounting specimen pieces in lucite and polishing and etching by standard procedures [21] to get the transverse cross section. For steel, the etchant was nital. Aluminum was etched by immersing in a solution of 1ml 48% hydrofluoric acid (HF) in 200ml water for 45s. Copper was etched in a solution of 20ml ammonimum hydroxide (NH_4OH), 20ml water and 20ml 3% hydrogen peroxide (H_2O_2) by immersion for 1 minute.

Scanning electron fractographs of the appearance of the fractured surfaces at various locations and magnifications were also taken to examine the nature of the fracture.

IV. RESULTS AND DISCUSSION

Shape Change Experiments

Rolling deformed the initially circular holes into approximately elliptical ones, with the eccentricity of the ellipse increasing with successive rolling passes. Type A specimens were reduced in thickness by 50% in 6 passes. A typical sequence is shown in Fig. 13. Type B and type C specimens were reduced 35% in 3 passes. A typical sequence is seen in Fig. 14. The length of the major and minor semiaxes of the holes were measured after each pass. Since it is to be expected that a defect filled with relatively soft material will plastically deform such that its volume remains constant, it is reasonable to assume that the same result will hold approximately for a void.

If this is the case,

$$\pi r^2 h_o = \pi ab h_1$$
$$ab = \left(\frac{h_o}{h_1}\right) r^2 \qquad (1)$$

where

r = initial hole radius as drilled

a,b = major and minor semiaxes of ellipse

ho = initial thickness of specimen

h_1 = thickness after rolling.

Experimental values of ab (averaged over the holes in a given specimen and material) plotted against the theoretical value of ab

from equation (1) for the three materials and a range of values of $\frac{h_0}{h_1}$ from 1.19 to 2.10 are shown in Fig. 15. The trend is linear with a tendency to dip at higher levels of reduction suggesting the volume does reduce at very high reductions. Chaaban and Helmi's work [17] with plasticine shows complete closure of all the 3 kinds of holes they considered (vertical, longitudinal and transverse) beyond a certain amount of reduction. Both [17] and [18] report a variation in the amount of area change across the cross sectional width and depth and across the length of the specimens. The experiments performed in this thesis work dealt only with vertical holes. However, for upto 50% reduction, no appreciable dependence of shape or area on the position of the holes along the width was seen, except in the case of steel. For steel, a variation of hole area was seen as a function of the hole position along the width, with hole area increasing for holes near the center and decreasing for holes close to the edges of the specimen. This is shown in Fig. 16.

A possible explanation for this variation could be that only steel is strong enough to cause an appreciable variation of roll pressure across the specimen width owing to a slight elastic deflection of the rolls. References [22-23] consider the variation of normal pressure p and the coefficient of friction μ in the compression of metal disks with and without lubrication. From Fig. 17, taken from [22], it is seen that μ is smaller when p is bigger. Also, from the details of the ring compression test in [19], we see that the change in internal diameter of an annular ring being compressed is a function of interface friction - with increasing

friction, the diameter expands as though it were part of a solid cylinder, but with diminishing friction, free inward radial flow is no longer obstructed and the internal diameter starts to reduce. A roll pressure variation with a minimum pressure at the center and larger pressures along the width away from the center would cause a variation of the coefficient of friction with a minimum near the edges and maximum towards the center. Then, similar to the ring test, the hole would tend to expand where the friction is high and contract where the friction is low and this is just what is observed. That this is not seen in aluminum or copper is attributed to the fact that they are not strong enough to cause appreciable roll deflection and roll pressure variation in the axial direction.

Equation (1) is but one expression for the two variables a and b. Several attempts were made to obtain a second relation involving a and b but without success. However, the ratio a/b when plotted against the reduction in thickness R (%) is reasonably approximated by a single curve (Fig. 18). The ratio of a/b is found not to be particularly material-sensitive. Values of a and b may be estimated for any value of reduction (R) by using (1) and the empirical curve of Fig. 18.

Interaction of Adjacent Defects

In practice, soft defects are present in groups rather than in isolation, and these groups may interact with each other relative to change in shape and concentration of stress. This problem was initially considered by rolling a specimen of the type in Fig. 7

where a square defect arrangement was considered in a 5 x 5, 3 x 3 and 1 x 1 matrix arrangement. In all the cases the deformation of the center hole was measured. It was seen that the 1 x 1 center hole was bigger than the 3 x 3 center hole but the latter and the 5 x 5 center holes had identical dimensions pass after pass, suggesting that the holes immediately adjacent to the central hole significantly influence the deformation of the central hole while those in the next more distant position have only a weaker or "second order" influence on the deformation. It was therefore concluded that it would be sufficient to include only defects immediately adjacent to the central one when studying interactions. The ligament spacing relative to the hole size would of course be an important variable in any interaction study. Since the interaction question was somewhat removed from the main thrust of this study, it has not been pursued further but it seems clear that it should be considered in detail if the role of soft inclusions on the brittle fracture characteristics of metals proves to be of sufficient importance. As a result, only the characteristics of a single hole were studied in the subsequent experiments.

Fracture Experiments

The results obtained that are material-specific are listed first, followed by a summary and discussion of the general characteristics seen in all the materials. See Table 4.

OFHC Copper: As expected, it exhibited the maximum ductility (up to 60% was recorded) and also a lot of strain hardening, for it

shows a sizeable difference between the ultimate tensile strength in the annealed and in the strain hardened, cold worked state. A typical load-displacement curve is seen in Fig. 19. The annealed specimens all exhibit a "tensile" type failure where the fracture surface is normal to the loading direction. Half the B specimens were not annealed and they exhibit necking in two directions in the plane defined by the longitudinal and the width direction; these two directions intersecting each other and symmetrically making about 35° on an average with the width direction. (Fig. 22)

Al 5052: This alloy contains solutes like magnesium and owing to this, the specimens exhibit a dynamic strain-aging behavior with a serrated stress-strain curve (Fig. 20) which is obviously the Portevin-LeChatelier effect, described in [1], in action. "The serrations arise from successive yielding and aging when the specimen is tested. If the speed of a dislocation line is slow, it may be able to move by dragging its atmosphere of impurities along with it... At higher velocity, the dislocation pulls away from the atmosphere and a yield drop occurs. Since solute atom mobility is high at the temperatures at which discontinuous yielding occurs, new atoms move to the dislocations and lock them. The process is repeated many times, causing the serrations in the stress-strain curves."

The aluminum specimens exhibit the least ductility as well as small strain hardening. Here some of annealed specimens exhibited a "tensile" fracture as discussed for copper and some showed a "shear"

fracture with a shear failure in the length-thickness plane at 45° to the length direction and normal to the width direction. (Fig. 22) All the non-annealed B specimens failed at about 35° as discussed for copper.

ST 1018:

The specimens all exhibit typical yield-point phenomena, with upper and lower yield points and Luders band formation, as seen in Fig. 21.

The steel specimens, as expected, have the highest tensile strength.

The following common characteristics are observed:

1. The central defect, which may be a circle or ellipse (depending on whether the hole was drilled after or before rolling) with major axis parallel or transverse to the direction of loading, undergoes a substantial change in shape during the tension test. The change is always towards an ellipse with major axis in the loading direction.
2. Two types of necking are observed (Fig. 23). Necking in the width direction is diffuse while that in the thickness direction is localized. In the unannealed specimens with holes in them, two localized necks form that intersect each other and make about 35° with the width direction. In some of the unannealed specimens without holes in them, only one such oblique neck is formed instead of two. This appears to be a surprising result but it turns out to have been noticed and reported as early as

1928 by Koerber and Siebel [24]. (See Fig. 24). Hill [25] developed plastic stress-strain rate relations satisfying the anisotropy of a cold-rolled flat bar and computed the angle for the oblique straight direction along which a bar of anisotropic material contracts before fracturing. Nadai [26] states it this way: "It is well known to testing engineers that wide flat bars or strips machined from thin rolled metal sheet when tested in cold worked condition in tension do not break in a surface which is perpendicular to the direction of tension but along an oblique plane perpendicular to the flat sides of the bar inclined at an angle of approximately 55 degrees with respect to the axis of the bar..... the flat bars must have a ratio of width to thickness of the rectangular section larger than 6 or 7 otherwise they neck down symmetrically around a section normal to the bar axis." Koerber and Siebel attribute this type of fracture to a simultaneous gliding in the metal on two systems of slip planes.

The mathematical derivation of the 55° angle as presented by Nadai [26] is discussed in the Appendix. It is based on finding that oblique direction with respect to the tensile axis in which no normal strains are produced under simple extension. Shaw and Avery [27] have followed similar agruments but used Mohr's circle of strain in the plane stress situation to obtain the same result. Nadai suggests that two slip layers symmetrically inclined with respect to the axis form, intersecting each other in the weaker region if there is such a

region in the interior of the bar. This is certainly true in the case of the specimens with the holes in them and as expected, all the unannealed specimens of all the materials with holes in them form two intersecting slip layers and fracture randomly along one of them.

3. The results indicate that the UTS, which is always calculated based on the sound area at the central crosssection before the tension test, is insensitive to the shape or orientation or size of the hole. This can be explained by the fact that large plastic flow around a void in a ductile material wipes out the effect of hole shape and orientation and reduces the elastic stress concentration effect to a negligible value. Ramanath [28] has used the ANSYS Finite Element Program to calculate the stress distribution in a plate with a round hole in it subjected to uniaxial tension, before and after yielding occurs at the stress concentration viz. the hole. The specifics of the problem he considered are:

   Rectangular plate 10" x 6" x 0.1" with a 2" diameter hole in the center.

   Young's Modulus (E) = 30×10^6 psi

   Poisson's Ratio (ν) = 0.3

   Yield Strength (σ_{yp}) = 90,000 psi

   Slope of flow curve = 0.032

   Since the problem is symmetric the results are presented for only 1/4 of the plate in Fig. 25. The curves on the figure denote lines of constant normal stress. From Fig. 25(a) which

pertains to the elastic stress immediately before yielding we see:

Maximum normal stress - - - - - - - - - - - $\approx$ 87,000 psi

Stress far away from stress concentrator $\approx$ 32,000 psi

This corresponds to an elastic stress intensification factor of about 2.7.

Figure 25(b) shows the state of stress a little after yielding:

Maximum normal stress - - - - - - - - - - - $\approx$ 101,000 psi

Stress far away from the stress concentrator $\approx$ 64,000 psi

This corresponds to a stress intensification factor of about 1.6 after yielding. Hence it is obvious that the stress intensification factor will drop further to a much lower value if the plate is subjected to large plastic deformations of the magnitude considered in the present work.

In other words, the maximum intensified stress theory of Takagi [2] does hold good for ductile materials but there is no difference between the nominal and the intensified normal stress. Strain at fracture is found to depend considerably on the orientation of the hole. Of all the defects, an elliptical defect with its major axis aligned with the direction of loading results in the most ductility. A round hole (before testing) yields intermediate ductility. Ductility is minimal if the major axis of the elliptical defect is transverse to the loading direction. Of course, specimens with no holes have the highest ductility. For ductile materials, the nominal stress fracture

criterion applies. For brittle materials, however, the shape effect of voids and defects is important and nominal and intensified stress must be distinguished between. The results on both stress and strain are in keeping qualitatively with the findings in [4-7], which dealt with the mechanical fibering of inclusions being the defect instead of the voids which have been considered here.

4. At maximum load, the initiation of a small crack is evident at the edges of any hole at points 90° from the load line. This crack grows rapidly with substantial necking, with further increase in deformation as the load rapidly falls to zero.

5. One common feature which was observed in all the specimens with holes in them was that they necked well before the maximum load was reached whereas in a regular tensile specimen without a hole and subjected to uniaxial tension, the theory [1] states that instability occurs when

$$dP = 0$$

where P is the applied load.

This requires that the load be a maximum when necking starts. The explanation for this is the triaxiality of stress that is induced at an early stage owing to localized yielding at the hole, which is a stress concentrator.

6. The fracture surface appearance is seen in the Scanning Electron Microscope fractographs of Fig.26. In all the 3 cases clear cut ductile dimple fracture is seen with roughly equiaxed grains and some shear flow near the edges.

V. CONCLUSIONS

1. The presence of shaped voids and their size and orientation has a very significant effect on the strain to fracture of the metals studied. The presence of the hole reduces the strain to fracture relative to the tensile stress because once yielding begins, the hole effectively reduces the gage length.

   While the ductility in an anisotropic material significantly depends on the direction in which the specimen is cut, the tensile stress has been found not to be direction dependent. Mehl and co-workers [4-7] have highlighted the first part of this statement but it is felt that the second part is quite as important, as in the situation where obtaining large strains is important while the stress levels are of secondary importance. For instance, in the case of automobile bodies which are made by sheet-metal working it is highly desired to obtain the maximum plastic strain at the same stress level. It was attempted in the course of this study to see if putting in a pattern of hemispherical dimples on one side of a sheet-working specimen would increase the plastic flow to fracture when the specimen was rolled. This experiment was not successful. It failed in two ways. One, that even the lightest dimple indented on one side of the sheet resulted in blemishes on the other side. This has been reported earlier by Johnson [29]. The other was that the very presence of the dimple made it less ductile than a specimen with no dimples.

2. Annealing has the effect of removing the anisotropy due to cold working. Annealed specimens fail normal to the applied load while cold-worked samples with a large width to thickness ratio ($\sim$16 in this study) are found to fracture obliquely owing to the reasons discussed in Chapter IV.
3. It is found that the ultimate tensile strength of the metals studied is not affected significantly by the presence of holes, owing to plastic flow and consequent disappearance of stress intensification. The hole only has the effect of reducing the sound area of the specimen and hence the maximum load bearing capacity while the UTS is unaltered. The maximum intensified stress criterion which applies to brittle materials is also found to apply to ductile materials but since in ductile materials the stress intensification factor is roughly equal to 1, the intensified stress criterion reduces to a maximum nominal stress criterion.
4. In the shape change experiments, all the holes change uniformly in area, the governing criterion being the constancy of volume of the hole.
5. Only in the case of steel, the holes close to the edges of the specimens decrease in area, and hence in volume, upon rolling. This is explained to be due to a roll pressure gradient in the roll axis (i.e. the specimen width) direction, upon which is attendant an axial direction gradient of coefficient of friction. This could possibly be uesd as a rolling mill stiffness acceptance test where a specimen of steel with several

vertical holes along its width is rolled in plane strain in the mill and the variation of hole size change across the width is measured. For the stiffness of the mill to be acceptable, the variation in hole size change would have to be less than a certain limit.

6. Tensile specimens with holes in them are seen to neck always before maximum load is reached, owing to the triaxiality of stress introduced early by the presence of the hole.

Table 1

Material properties (Annealed Condition)

Material and Composition	Flow stress ksi (MPa)	UTS ksi(MPa)	Elongation (%)	q (%)	Annealing temperature (°C)
1. OFHC Cu (99.99%Cu)	10 (70)	32(220)	50	78	375-650
2. Al 5052 (2.5% Mg)	13 (90)	28(190)	25	-	340
3. AISI 1018 (0.18%C) steel	44 (300)	65(450)	35	70	850-900

Table 2

Rectangular tensile specimen dimensions

Specimen type	Number of pieces with elliptical holes		Number of pieces with round holes		Number of pieces with no holes		G in. (mm)	W in. (mm)	R in. (mm)	L_o in. (mm)	A in. (mm)	B in. (mm)	C in. (mm)
	L	T	L	T	L	T							
A	5	5	4	4	-	-	1.250 (31.75)	0.250 (6.35)	0.250 (6.35)	4.000 (101.6)	1.500 (38.1)	1.250 (31.75)	0.375 (9.525)
C1	6	-	4	-	2	-	3.000 (76.2)	0.800 (20.32)	0.750 (19.05)	6.800 (172.72)	3.800 (96.52)	1.500 (38.1)	1.000 (25.4)
C2	4	-	2	-	2	-	2.250 (57.15)	0.600 (15.24)	0.600 (15.24)	5.800 (147.32)	3.000 (76.2)	1.400 (35.56)	0.800 (20.32)
C3	4	-	2	-	2	-	1.750 (44.45)	0.400 (10.16)	0.400 (10.16)	4.750 (120.65)	2.250 (57.15)	1.250 (31.75)	0.600 (15.24)
C4	4	-	2	-	2	-	1.250 (31.75)	0.250 (6.35)	0.250 (6.35)	4.000 (101.6)	1.500 (38.1)	1.250 (31.75)	0.375 (9.925)

L -- Longitudinal Specimen
T -- Transverse Specimen
T_o -- Thickness of material as rolled
0.065 in. for type A specimens
0.080 in. for type C specimens

Table 3

Distribution of plane strain tensile specimens

	Longitudinal with elliptical hole	Transverse with elliptical hole	Longitudinal with round hole	Transverse with round hole	Longitudinal with no hole	Transverse with no hole
Number of pieces	4	4	2	2	2	2

Table 4

Results of tensile tests

Material	Specimen type and condition	Specimen Numbers	Ultimate Tensile Strength (ksi)	Elongation (%)	Reduction in area (%)	Type of fracture
OFHC Copper	A-0	T1-T5	34	10	21	I
		T6-T9	34	17	35	I
		L1-L5	34	24	59	I
		L6-L9	34	17	36	I
	B-0	T	33	53	59	I
		L	32	59	67	I
		No hole	32	85	70	I
	B-1	T	53	17	43	II
		L	55	26	57	II
		No hole	54	50	42	II
Al 5052	A-0	T1-T5	29	4	10	I
		T6-T9	29	7	15	I
		L1-L5	30	10	18	I
		L6-L9	30	7	14	I
	B-0	T	34	23	26	I, III
		L	34	21	27	II
		No hole	35	24	46	I,III
	B-1	T	40	12	22	II
		L	38	12	20	II
		No hole	40	12	32	II
St 1018	A-0	T1-T5	48	3	16	III
		T6-T9	48	12	17	III
		L1-L5	47	12	21	III
		L6-L9	47	11	15	III
	B-0	T	71	28	51	II
		L	68	37	51	II
		No hole	68	44	50	II,III
	B-1	T	77	19	32	II
		L	69	28	46	II
		No hole	70	22	46	II
	C1-0	L	63	21	41	III
		No hole	63	32	56	III
	C1-1	L	119	3	22	II
		No hole	118	3	27	II
	C2-0	L	66	20	42	III
		No hole	63	30	55	III
	C2-1	L	118	4	20	III
		No hole	118	5	28	III
	C3-0	L	69	17	43	III
		No hole	65	32	61	III
	C3-1	L	128	2	7	III
		No hole	118	11	40	III
	C4-0	L	68	14	53	III
		No hole	60	31	46	III
	C4-1	L	124	2	10	III
		No hole	120	8	17	III

0 — Annealed state
1 — Cold worked state
T — Longitudinal axis of specimen transverse to rolling direction
L — Longitudinal axis of specimen parallel to rolling direction
I — Tensile fracture perpendicular to applied stress
II — Fracture at 35° to long transverse direction
III — Shear fracture at 45° to short transverse direction

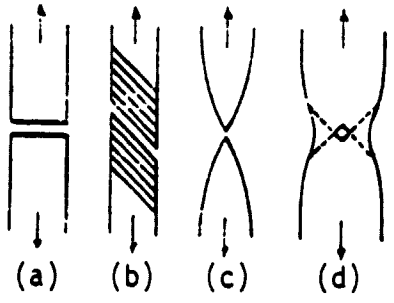

Fig. 1 Types of fractures observed in metals subjected to uniaxial tension. (1)

a)Brittle fracture of single crystals and polycrystals

b)Shearing fracture in ductile single crystals

c)Completely ductile fracture in polycrystals

d)Ductile fracture in polycrystals

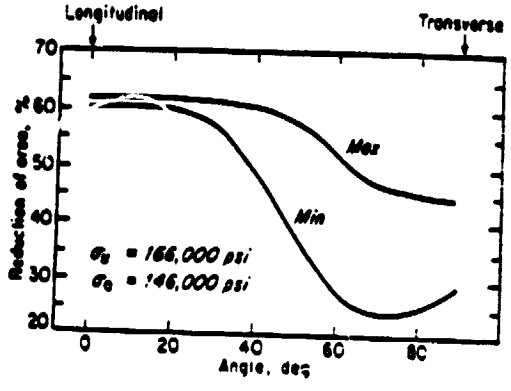

(a)

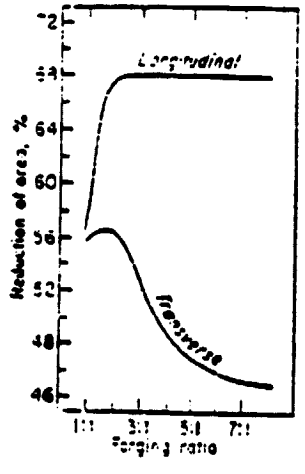

(b)

Fig. 2 Anisotropy of mechanical properties. (4)

a)Relationship between reduction of area and angle between the longitudinal direction in forging and specimen axis

b)Effect of forging reduction on the transverse reduction of area

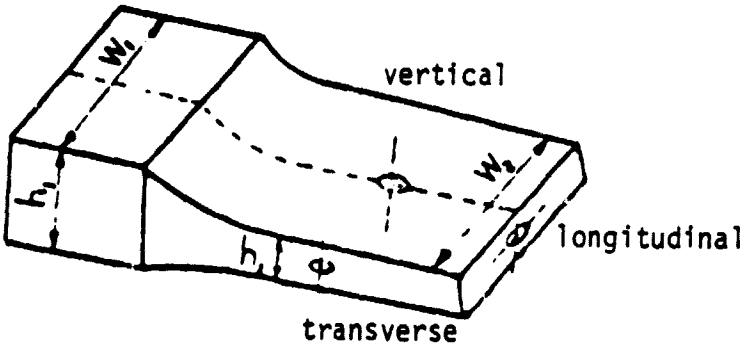

Fig. 3 Position of three kinds of holes. (17)

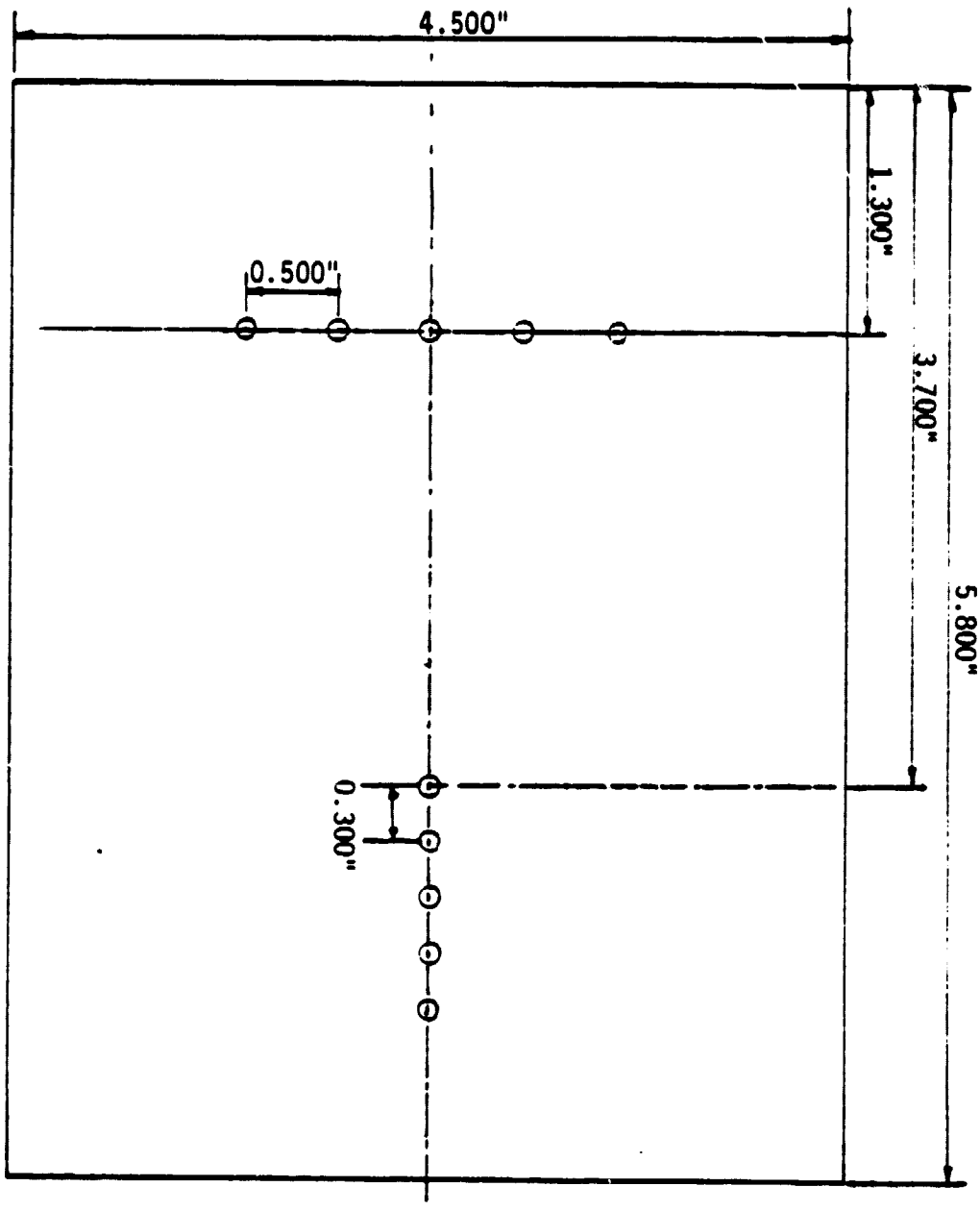

Fig. 4 Shape change specimen-Type A

All holes 0.040" dia. drilled and reamed

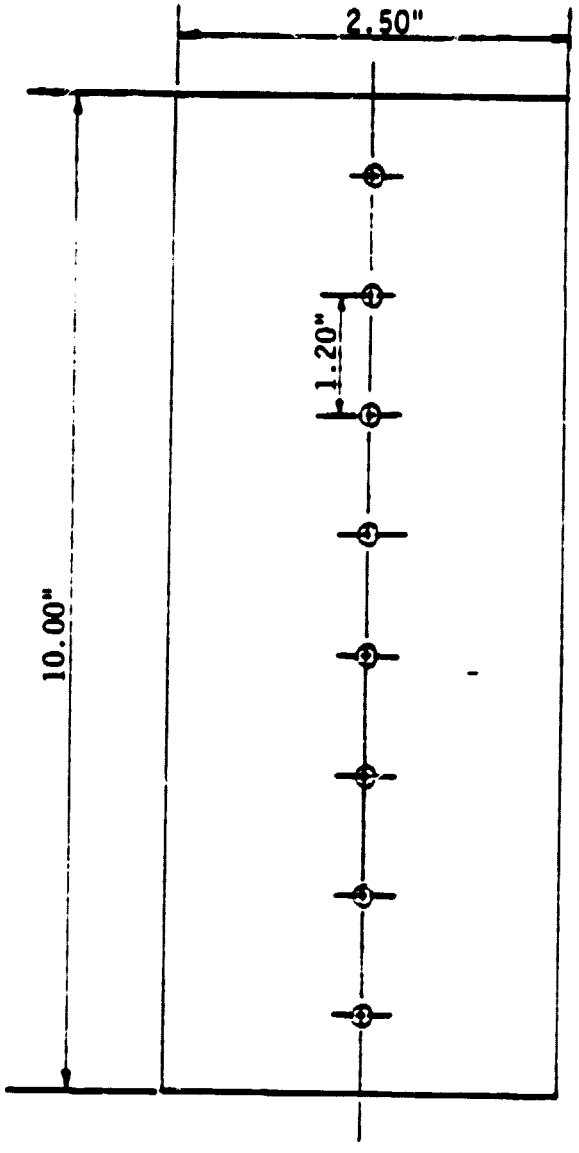

Fig. 5 Shape change specimen-Type B

All holes 0.040" dia. drilled and reamed

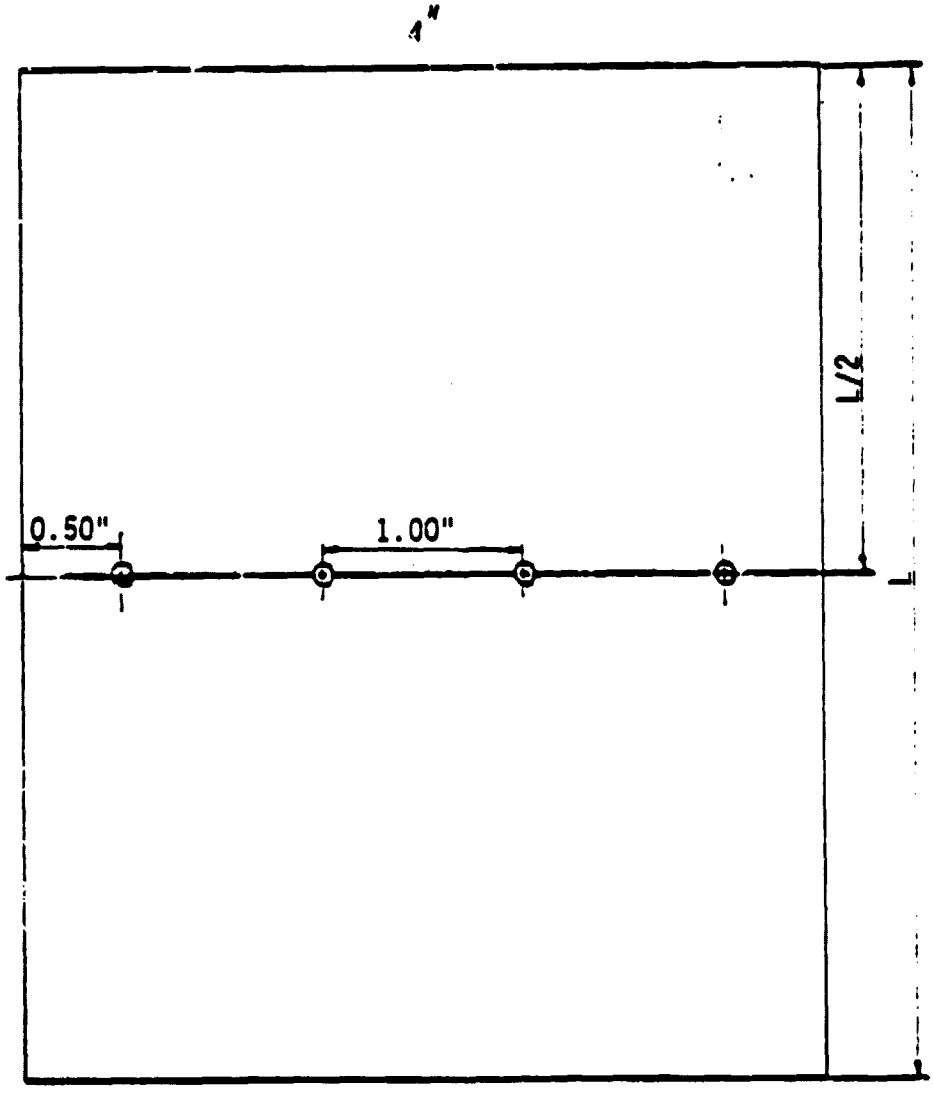

Fig. 6 Shape change specimen-Type C

All holes 0.040" dia. drilled and reamed

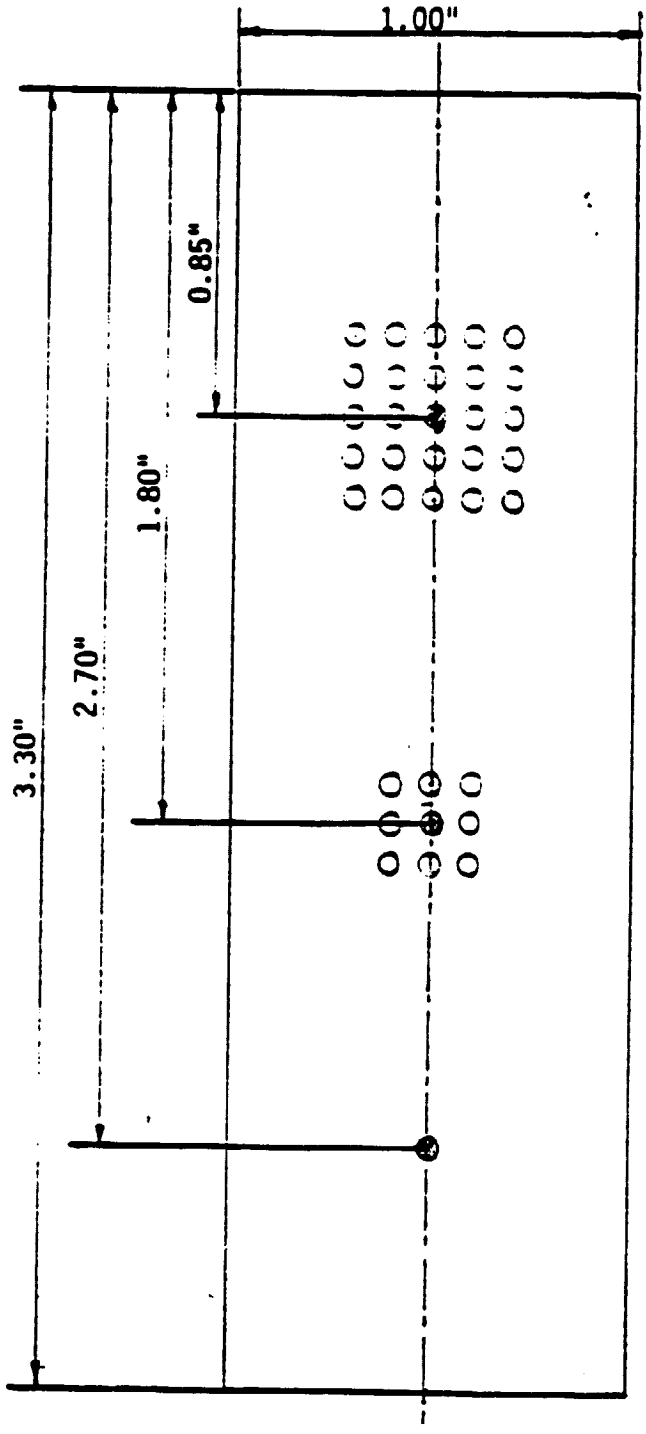

Fig. 7 Specimen to study interaction of adjacent defects.

All holes 0.040" dia. drilled and reamed
Hole spacing = 0.100"

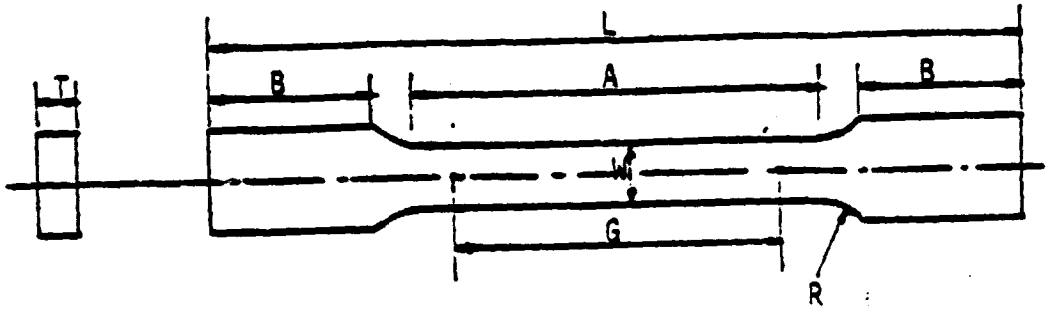

Fig. 8 Rectangular tensile specimen. (20)

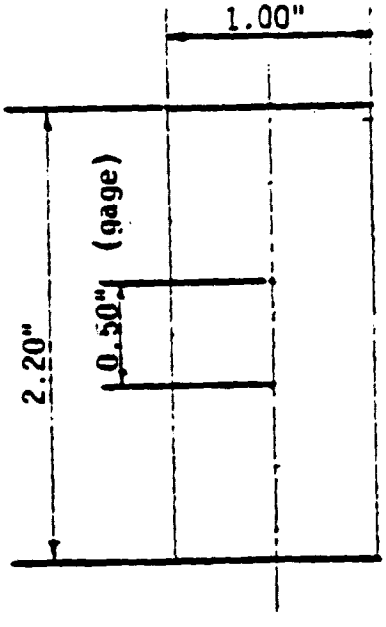

Fig. 9 Plane strain tensile specimen

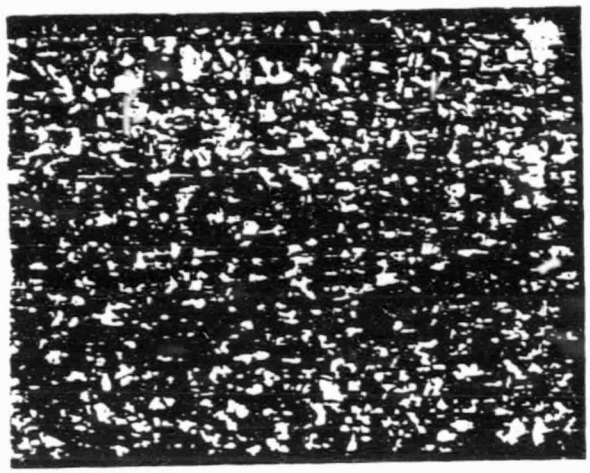

100X Etchant: NH_4OH, H_2O_2

(a)

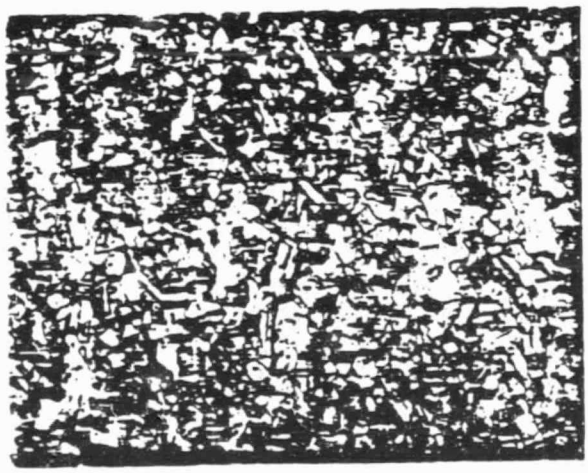

200X Etchant: NH_4OH, H_2O_2

(b)

Fig. 10 Microstructure of annealed OFHC Cu

a) Annealed, at 100X, showing fine grain structure

b) 200X. Twin boundaries are visible.

100X Etchant: HF in water

(a)

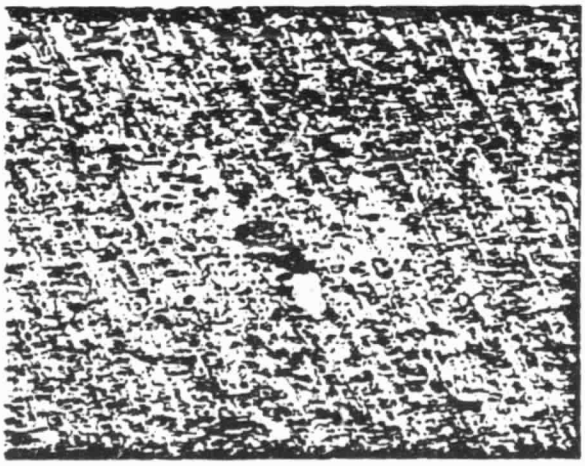

200X Etchant: HF in water

(b)

Fig. 11 Microstructure of annealed Al 5052

a) At 100X

b) At 200X, very fine grains and precipitates

100X Etchant: Nital

(a)

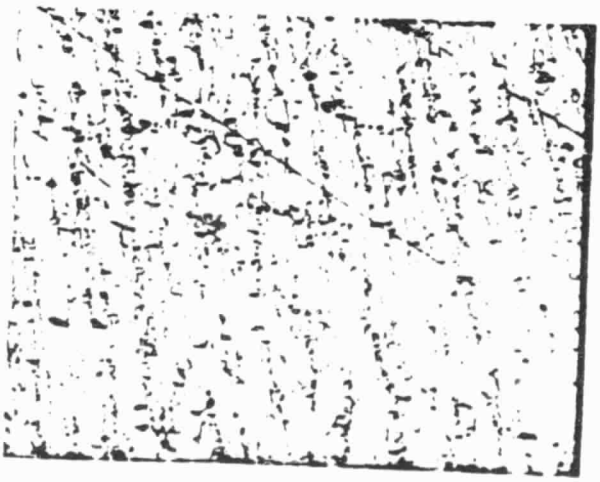

200X Etchant: Nital

(b)

Fig. 12 Microstructure of annealed steel AISI 1018

a) At 100X

b) At 200X. A lot of precipitates are seen

50X

(a)

50X

(b)

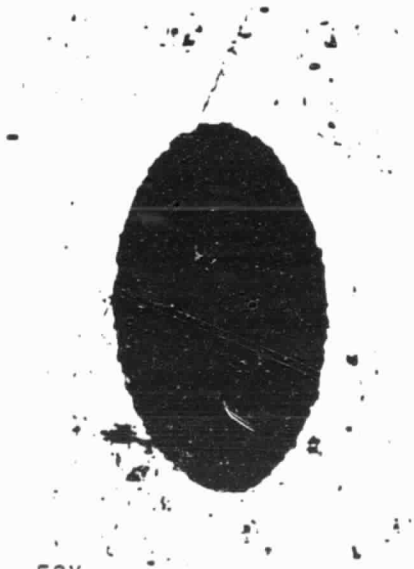

50X

(c)

50X

(d)

Fig. 13 Change of hole shape during rolling of A specimen (St. 1018)

a)Before rolling

b)After two passes

c)After four passes

d)After six passes

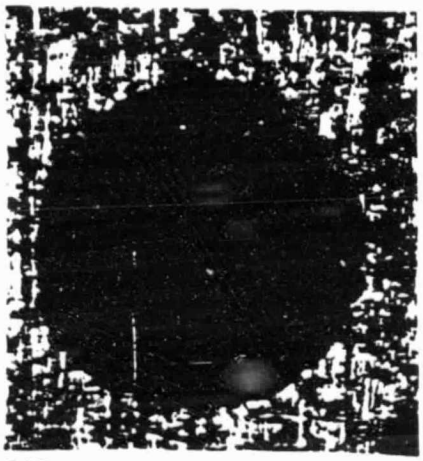

50X

(a)

50X

(b)

50X

(c)

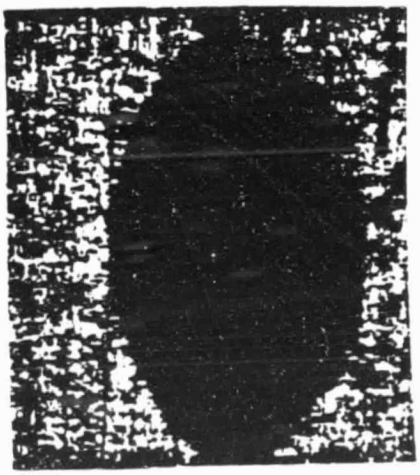

50X

(d)

Fig. 14 Change of hole shape during rolling of B and C specimens (OFHC Cu)

a)Before rolling

b)After one pass

c)After two passes

d)After three passes

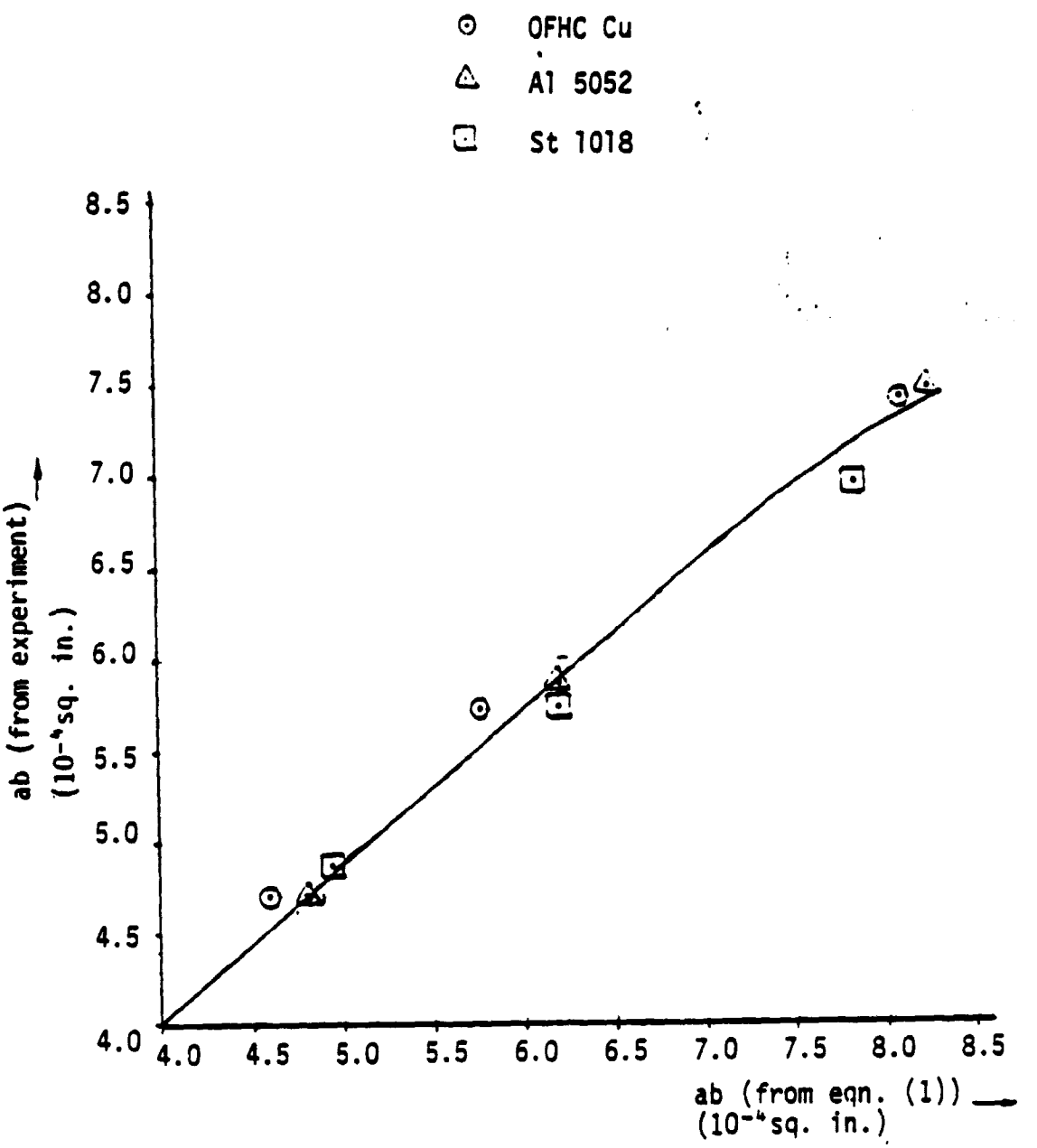

Fig. 15 Experimental values of ab vs. values from equation (1)

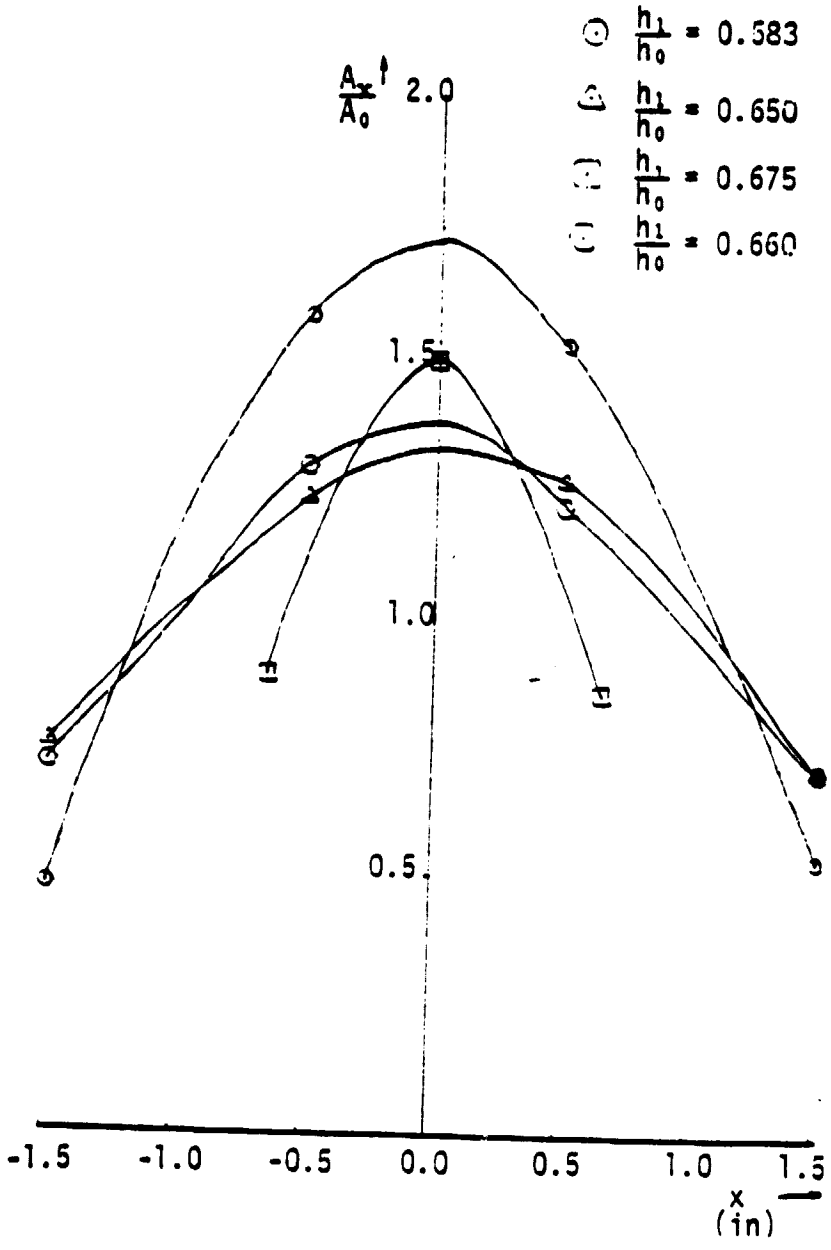

Fig. 16 Variation of hole shape change across width of specimen for steel.

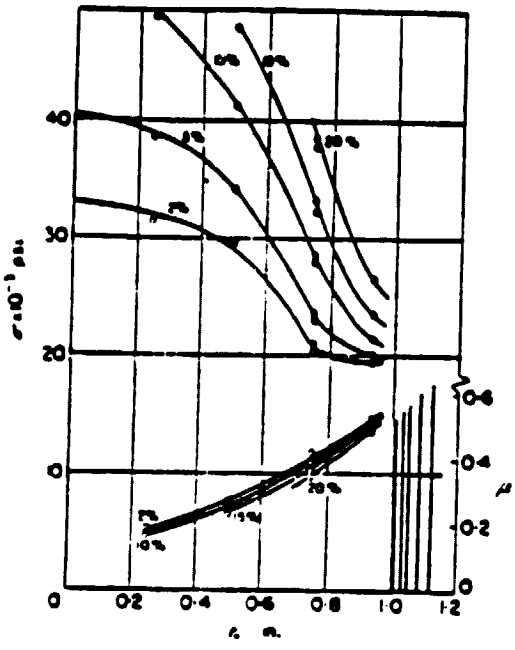

Fig. 17 Distribution of normal pressure and friction coefficient for various reductions on unlubricated aluminum, $\frac{d_n}{h_0} = 4.(22)$

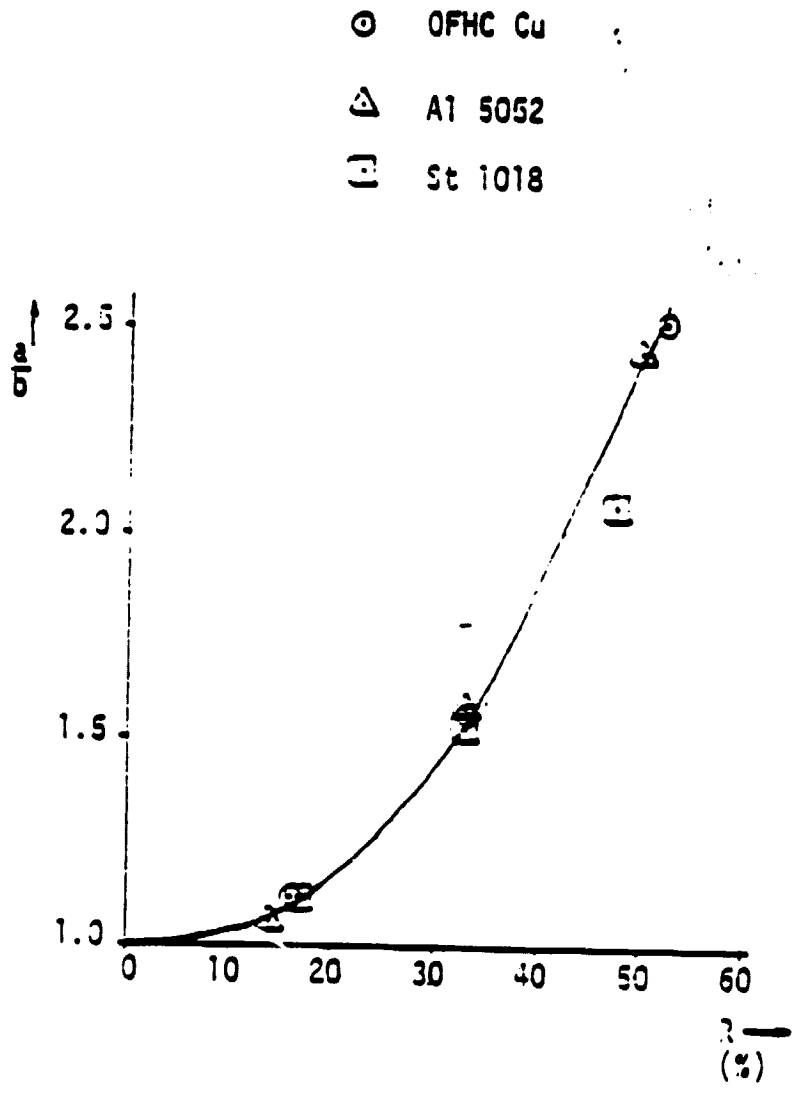

Fig. 18 Variation of ellipse eccentricity ratio (a/b) with percentage reduction in thickness (R).

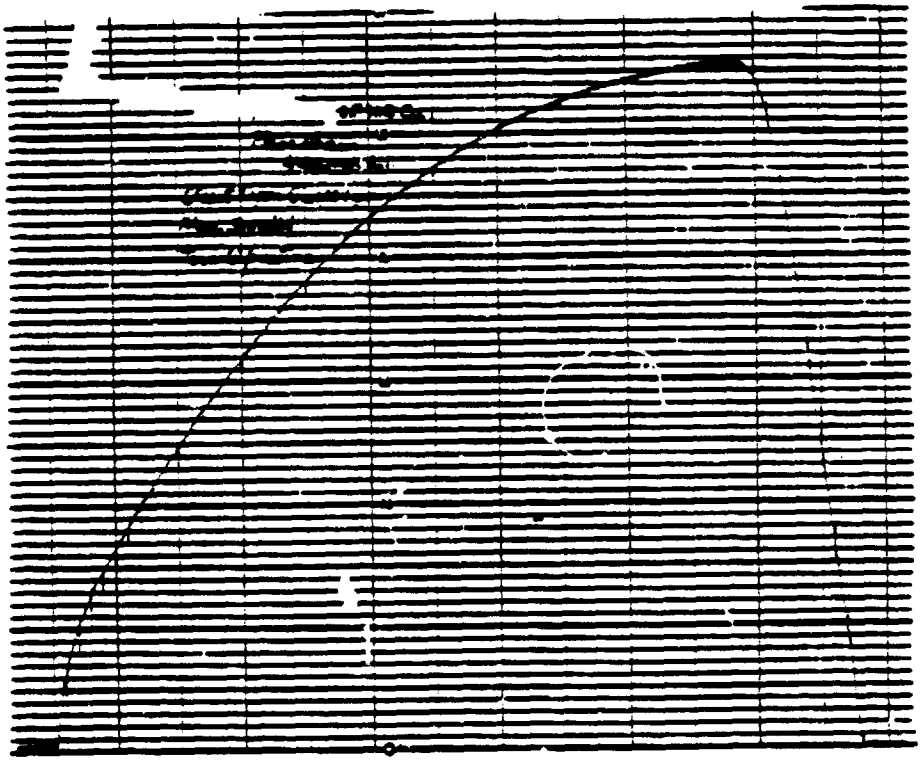

Fig. 19 Typical load-displacement curve for OFHC Copper

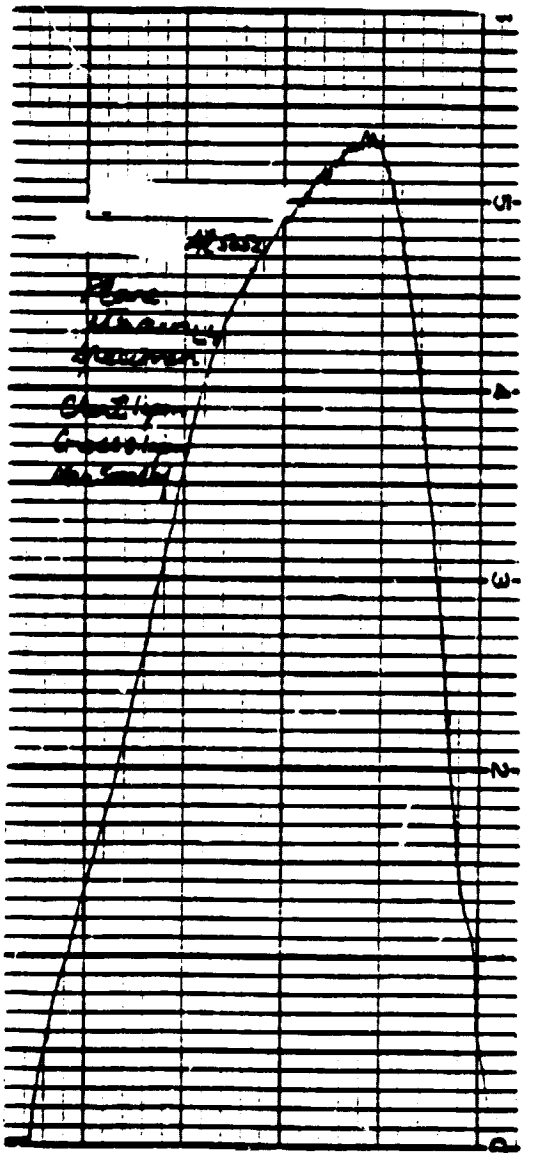

Fig. 20 Typical load-displacement curve for Al 5052

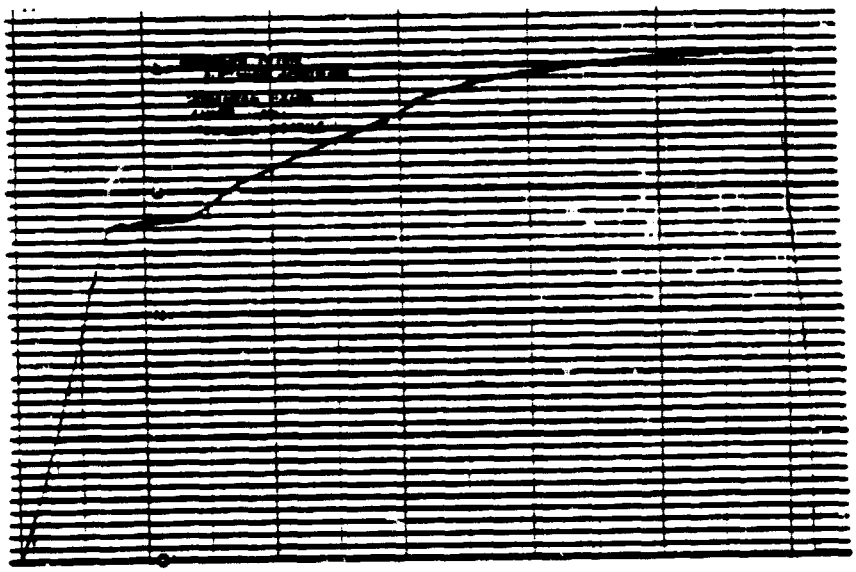

Fig. 21. Typical load-displacement curve for St 1018

FF -- Fracture line

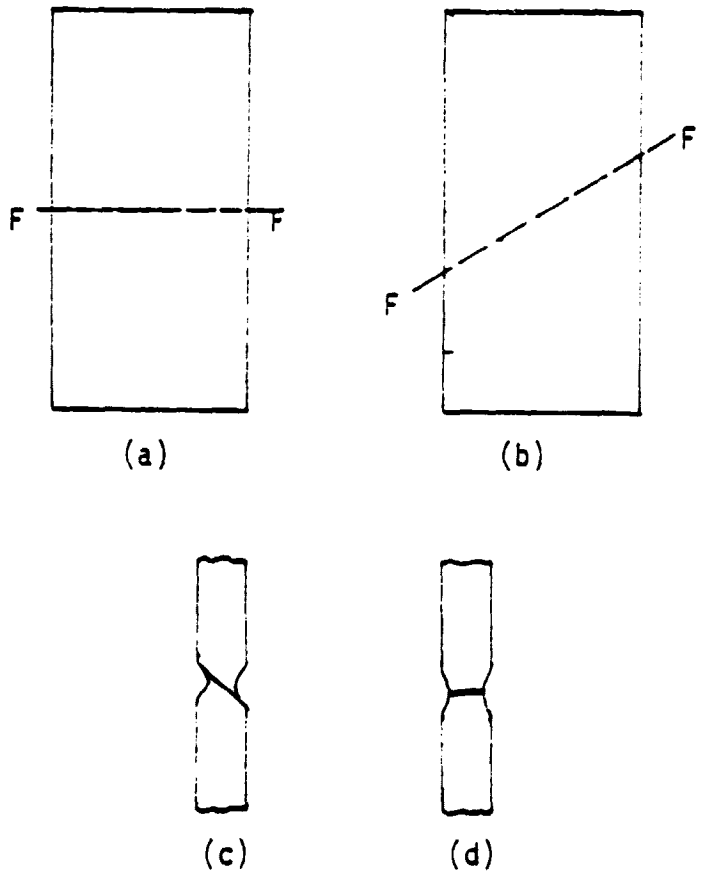

Fig. 22 Types of fracture observed

a) Normal fracture
b) Oblique fracture
c) Shear type fracture
d) Tensile type fracture

a) can occur in c) and d) modes
b) usually occurs in c) mode

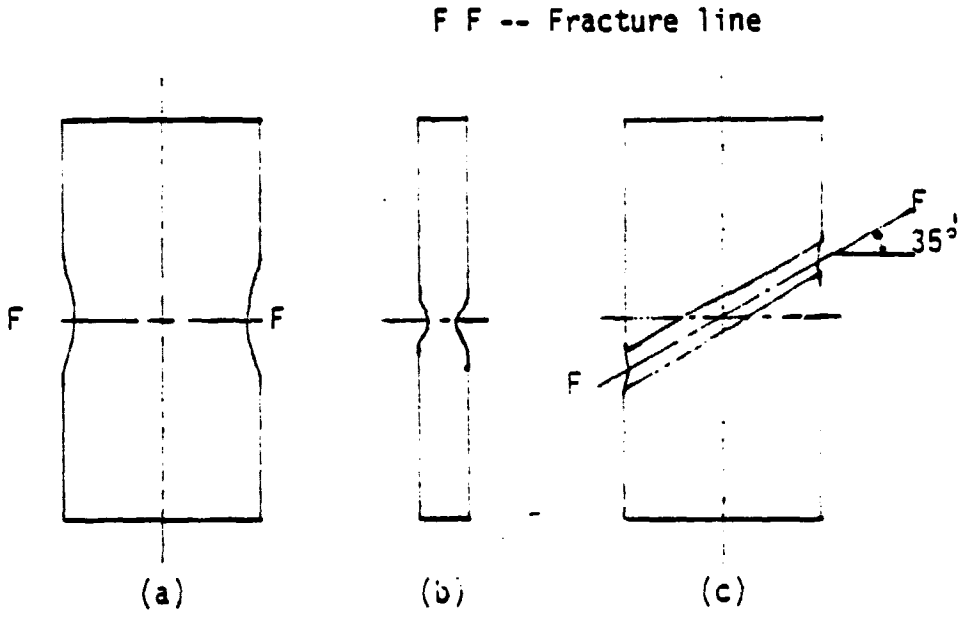

Fig. 23 Types of necking observed

a) Diffuse necking
b) Side view of a) showing localized necking
c) Oblique necking at 35°

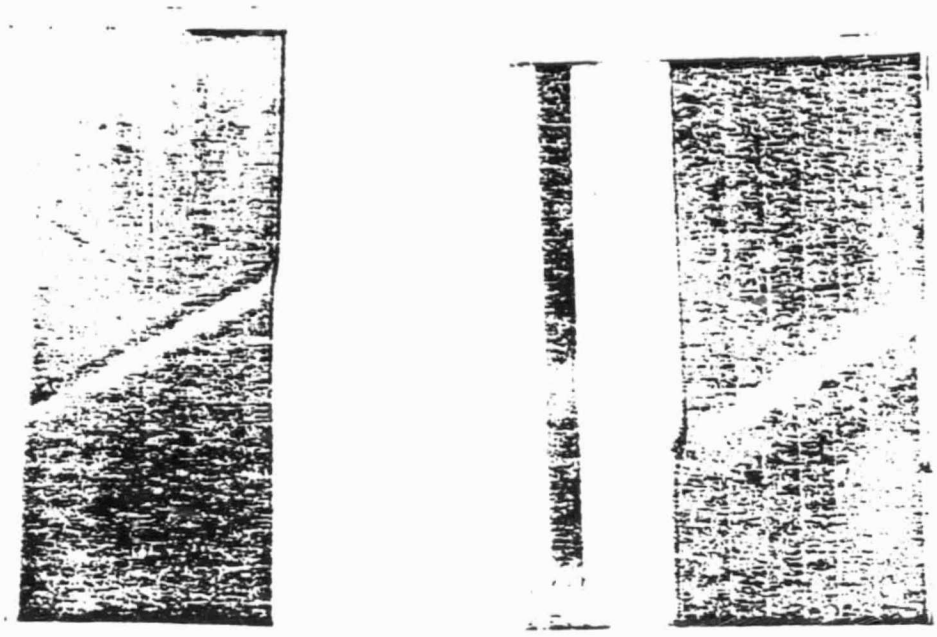

(a) (b)

Fig. 24 Necking along an oblique plane in flat steel bar tested in tension. (26)

a) Necking along an oblique plane in flat bar of cold-rolled low-carbon steel (ratio of width to thickness of cross section 16) tested in tension. (After Aronofsky)

b) Necking along an oblique plane in flat steel bar tested in tension. (The steel sheet was reduced in thickness by 20 per cent by cold rolling before the tensile test was made.) (After Koerber and Siebel)

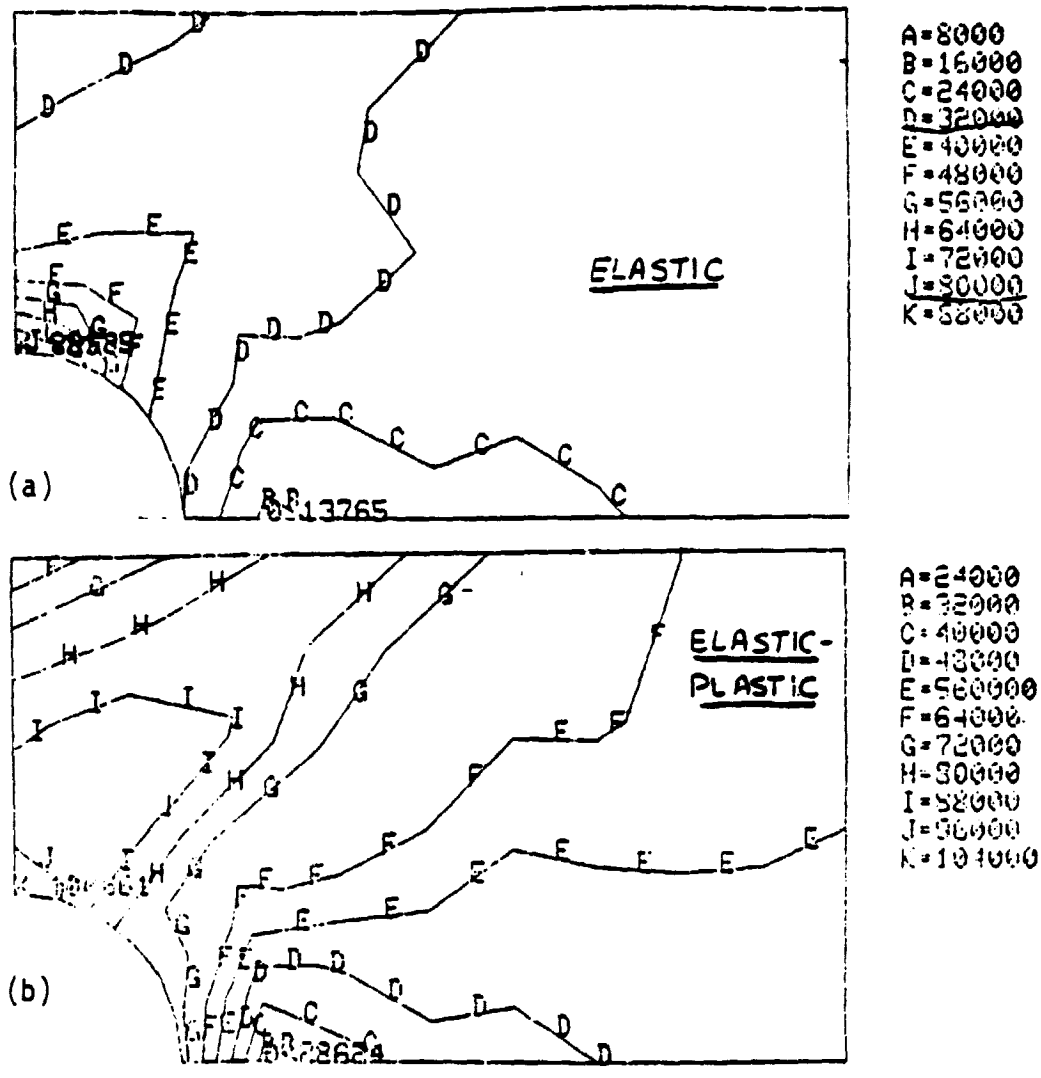

Fig. 25 Finite element solution of stress distribution in a plate with a round hole in it. (28)

a)Elastic region

b)After some yielding has occurred

(a)

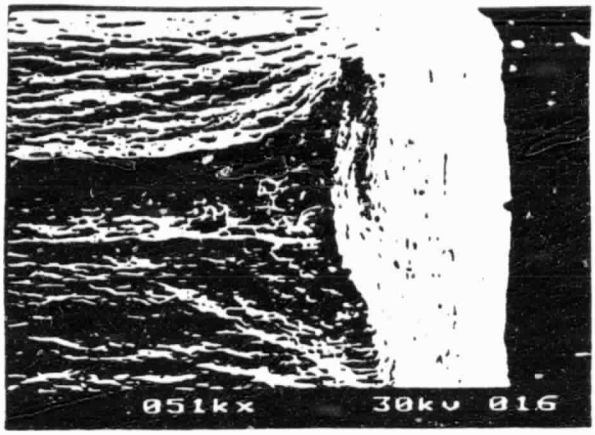

(b)

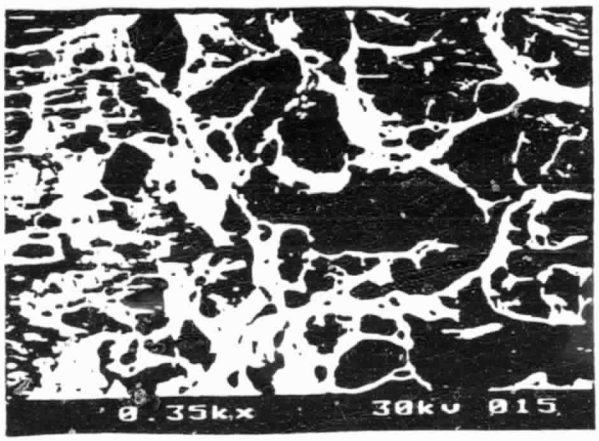

(c)

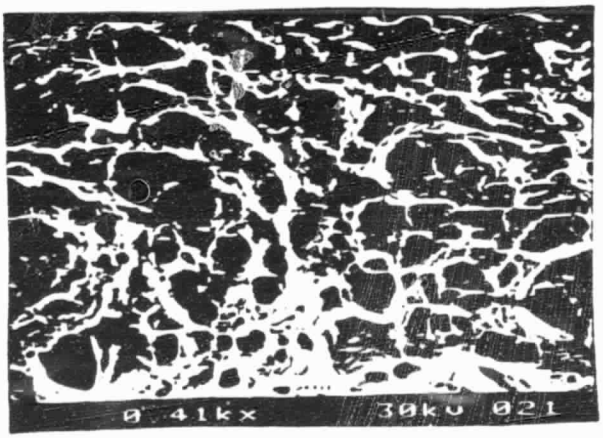

(d)

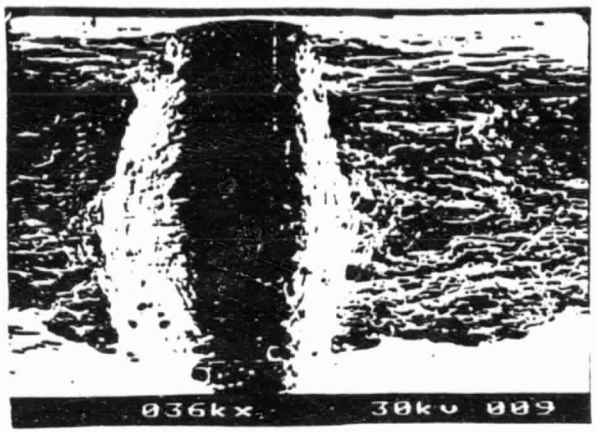

(e)

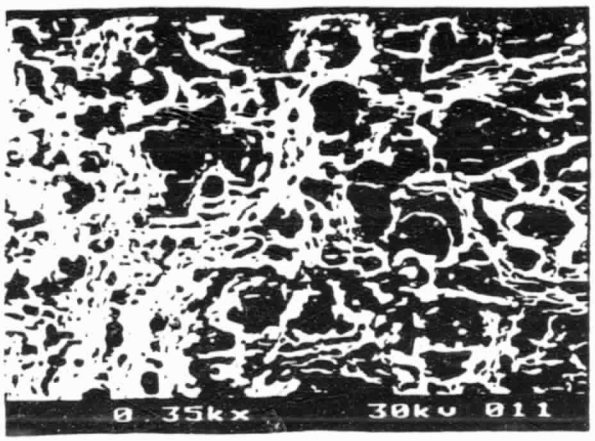

(f)

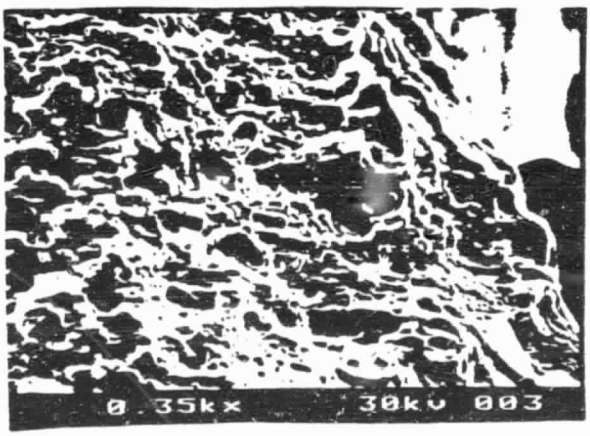

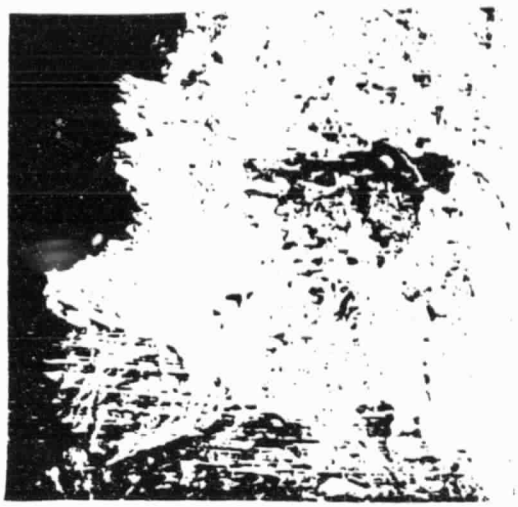

49X (g)

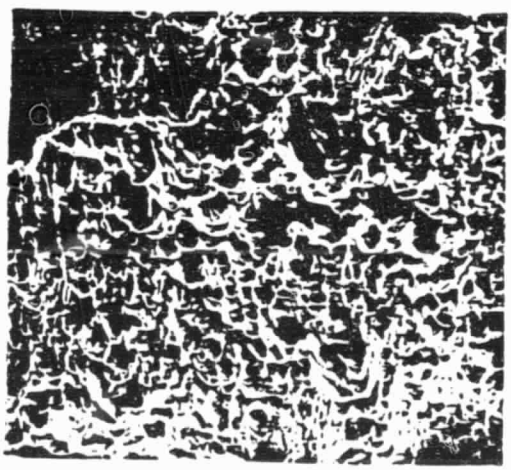

220X (h)

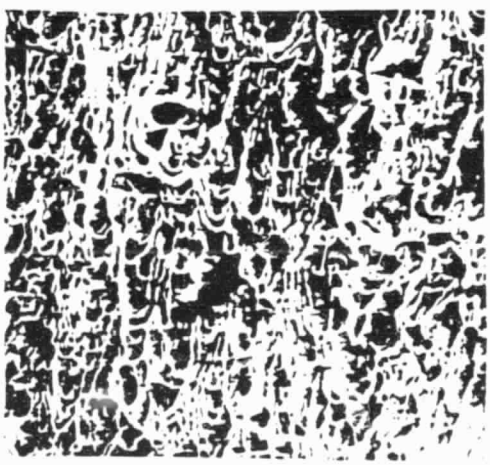

300X (i)

Fig. 26. Scanning electron fractographs of fracture surfaces
a), b), c) OFHC Copper. Note large, equiaxed dimples
d), e), f) Al 5052. Note equiaxed dimple pattern
g), h), i) St 1018. A lot more dimples are visible; slightly elongated; suggesting shear flow

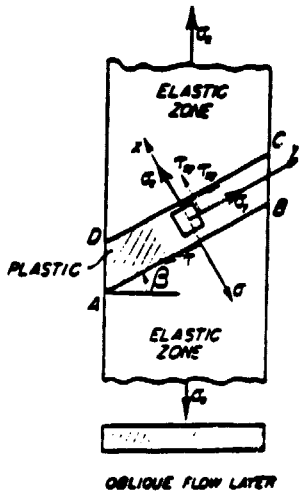

(a)

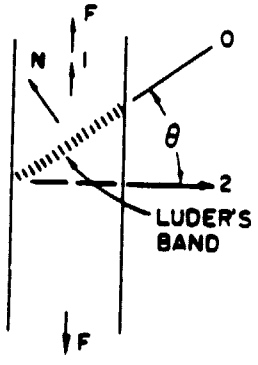

(b)

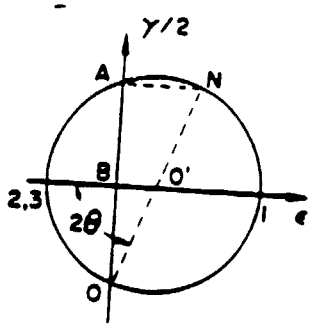

(c)

Fig. 27 Mohr's circle of strain for oblique necking

a)Oblique flow layer in wide flat tensile specimen. (26)

b)Luder's band in specimen (27)

c)Mohr's circle of strain for b). (27)

REFERENCES

1. Dieter, G.E., Mechanical Metallurgy, 2nd Edition, McGraw-Hill, New York, 1976.

2. Takagi, J., "Fracture of Brittle Materials," Dissertation, Arizona State University, Tempe, Arizona, 1981.

3. Griffith, A.A., "Theory of Rupture," Proc. First Int. Congress of Appl. Mechanics, Delft, 1924, pp. 55-62.

4. Wells, C., and Mehl, R.F., "Transverse Mechanical Properties in Heat Treated Wrought Steel Products," Trans. Am. Soc. Met., Vol. 41, 1949, pp. 715-818.

5. Grobe, A.H., Wells, C., and Mehl, R.F., "Transverse Mechanical Properties in an SAE1045 Forging Steel, "Trans. Am. Soc. Met., Vol. 45, 1953, pp. 1080-1122.

6. Loria, E.A., "Transverse Ductility Variations in Large Steel Forgings," Trans. Am. Soc. Met., Vol. 42, 1950, pp. 486-498.

7. Welchner, J., and Hildorf, W.G., "Relationship of Inclusion Content and Transverse Ductility of a Chromium-Nickel-Molybdenum Gun Steel," Trans. Am. Soc. Met., Vol. 42, 1950, pp. 455-485.

8. Backofen, W.A., Shaler, A.J., and Hundy, B.B., "Mechanical Anisotropy in Copper," Trans. Am. Soc. Met., Vol. 46, 1954, pp. 655-680.

9. McClintock, F.A., "On the Mechanics of Fracture from Inclusions," Paper presented at a Seminar of the American Society for Metals, October 1967, published in "Ductility," American Society for Metals, Metals Park, 1968, pp. 255-277.

10. O'Donnell, W.J., and Langer, B.F., "Design of Perforated Plates," ASME Journal of Engineering for Industry, Vol. 84, August 1962, pp. 307-320.

11. O'Donnel, W.J., "Effective Elastic Constants for the Bending of Thin Perforated Plates with Triangular and Square Penetration Patterns," ASME Journal of Engineering for Industry, Vol. 95 No. 1, 1973, pp. 121-128.

12. Goodier, J.N., "Concentration of Stress Around Spherical and Cylindrical Inclusions and Flaws," ASME Journal of Applied Mechanics, Vol. 55, 1933, pp. 39-44.

13. Sadowsky, M.A., and Sternberg, E., "Stress Concentration Around a Triaxial Ellipsoidal Cavity," ASME Journal of Applied Mechanics, Vol. 16, June 1949, pp. 149-157.

14. Edwards, R.H., "Stress Concentrations Around Spheriodal Inclusions and Cavities," ASME Journal of Applied Mechanics, Vol. 18, 1951, pp. 19-30.

15. Mirandy, L., and Paul, B., "Stresses at the Surface of a Flat Three-Dimensional Ellipsoidal Cavity," ASME Journal of Engineering Materials and Technology, Vol. 98, April 1976, pp. 164-172.

16. Johnson, W., and Mamalis, A.G., "A Survey of Some Physical Defects Arising in Metal Working Processes," Proceedings of the 17th Int. Mach. Tool Design Res. Conference, Birmingham, England, 1976, pp. 607-621.

17. Chaaban, M.A., and Helmi, A., "An Investigation into the Effect of the Geometric Factors on the Closure of Holes during Flat Rolling," Proceedings of the 17th Int. Mach. Tool Design Res. Conference, Birmingham, England, 1976, pp. 623-632.

18. Chaaban, M.A., and Alexander, J.M., "A Study of the Closure of Cavities in Swing Forging," Proceedings of the 17th Int. Mach. Tool Design Res. Conference, Birmingham, England, 1976, pp. 633-645.

19. Schey, J.A., Introduction to Manufacturing Processes, 1st Edition, McGraw-Hill, New York, 1977.

20. ASTM, "Standard Methods of Tension Testing of Metallic Materials," Annual Book of ASTM Standards, Part 10, ANSI/ASTM E 8-79a, 1980, p. 207.

21. ASM, Metals Handbook, 8th Edition, Vols. 7-8, American Society for Metals, Metals Park, 1972.

22. van Rooyen, G.T., and Backofen, W.A., "A Study of Interface Friction in Plastic Compression," Int. J. Mech. Sciences, Vol. 1, 1960, pp. 1-27.

23. Pearsall, G.W., and Backofen, W.A., "Frictional Boundary Conditions in Plastic Compression," ASME Journal of Engineering for Industry, Vol. 85, February 1963, pp. 68-75.

24. Koerber, F., and Siebel, E., "Zur Theorie der bildsamen Formanderung," Naturwissenshaften, Vol. 16, 1928, p. 408.

25. Hill, R., "A Theory of the Yielding and Plastic Flow of Anisotropic Metals," Proc. Roy. Soc. London, Ser. A, Vol. 193, 1948, pp. 281-297.

26. Nadai, A., Theory of Flow and Fracture of Solids, 2nd Edition, Vol. I, McGraw-Hill, New York, 1950, pp. 319-327.

27. Shaw, M.C., and Avery, J.P., "Forming Limits," ASME Journal of Vibration, Acoustics, Stress, and Reliability in Design, Vol. 105, April 1983, pp. 247-252.

28. Ramanath, S., unpublished work on finite element modelling of stress analysis using ANSYS, Arizona State University, Tempe, Arizona, 1982.

29. Johnson, W., "The Mechanics of Some Industrial Pressing, Rolling, and Forging Processes," Mechanics of Solids, The Rodney Hill 60th Anniversary Volume, Pergamon Press, Oxford and New York, 1982, pp. 303-356.

APPENDIX:

OBLIQUE NECKING

Nadai [26] states that the oblique necking should occur in wide flat bars of cold worked materials in that direction with respect to the tensile axis in which no normal strains need to be produced under a simple extension. This instability occurs in a band of material, called a Luder's band, in which the flow is plastic while the material on either side remains elastic [27]. See Fig. 27 (a) and (b). When deformation is continued, the specimen fractures in the same direction. In the initiation stage, the elastic material above and below the Luder's band has negligible strains in all directions including direction 0 in Fig. 27 (b). Hence, for the continuity of strain at the interface, the material in the Luder's band must have zero strain in the 0 direction. Now, if we consider the Mohr's circle diagram of strain for this loading situation, we see that point 0 corresponds to zero normal strain, and angle 2Θ in strain space corresponds to angle Θ in real space.

BIOGRAPHICAL SKETCH

Devdas Mizar Pai was born in [redacted] on [redacted]. He received his elementary education in Lucknow, India and his secondary education was completed in Madras, India. He entered the Indian Institute of Technology, Madras, India, and graduated in 1982 with a Bachelor of Technology degree in Mechanical engineering. In August 1982 he entered the Graduate College at Arizona State University in the field of Mechanical Engineering and has held a Research Assistantship in the Department of Mechanical and Aerospace Engineering. He is a member of Tau Beta Pi, a national honor society.